VI.9. FISCHER-TROPSCH CATALYSTS. ATTRITION OF CARBIDED IRON CATALYST IN THE SLURRY PHASE (Ram Srinivasan, Liguang Xu, Robert L. Spicer, Fred L. Tungate, and Burtron H. Davis).

VI.9.1. INTRODUCTION

Modern processing of ceramic and/or catalytic materials is improved by control of the particle(grain) size, as well as the shape, and the size distribution. In modern ceramic processing, the ultimate goal is to obtain dense microstructures of uniform grain size and shapes. Enhancements in physical and chemical properties in the end-products are made by controlling the particle/grain size, shape and size distribution.

Homogeneous microstructures can be obtained by utilizing mostly nanosize spherical particles (VI.9.1). Several industrial applications of ceramics require homogeneous and uniform microstructures (VI.9.2). For example, spherical alumina particles have proved to be very efficient as filters in rubber and plastic-based insulators, and as semi-conductor sealing materials (VI.9.3), as starting materials for plasma-sprayed wear-resistant coatings (VI.9.4-VI.9.6), as thermal barrier coatings (VI.9.4), and electrical-insulator coatings (VI.9.5). The control of particle size distribution is important in càtalysts since it has a significant effect on the surface area and the performance of the catalysts (VI.9.7-VI.9.11). The accuracy of the particle size data depends on the sample preparation, the particle shape and technique used for the particle size analyses.

A slurry phase reactor provides a greater advantage in the Fischer-Tropsch synthesis since it allows the heat generated during the very exothermic reaction t be handled more economically than in fixed bed reactors. For use in a slurry reactor, a

wax/catalyst separation is essential. For separations involving either filtration or gravity settling, the particles should be as large as can be suspended in the slurry by the gas/liquid velocities. A convenient method for preparing these large spherical particles utilizes spray drying.

An iron catalyst, following carbiding, may be less resistant to disintegration than the oxide catalyst. This is especially true for an unsupported iron catalyst. It was of interest to learn how rapidly the carbided catalyst attrited and how the catalyst spheres disintegrated. In the present investigation, the effect of abrasion during movement in a slurry on the particle size of a Fischer-Tropsch iron catalyst is analyzed.

VI.9.2. EXPERIMENTAL

The iron oxide catalyst UCI-1185-78 used in the present investigation was prepared by United Catalysts, Inc. (UCI), Louisville, KY. A spray drying technique was used to produce spherical shaped particles. The catalyst was calcined in air at 375°C following spray drying. Approximately 100g of the finished catalyst was placed in a plug flow reactor and pretreated with carbon monoxide. The catalyst was heated to 275°C at a rate of about 2°C/min., and then held at this temperature for 24 hours. CO flow was about 200 cc/min. and at a pressure slightly higher than atmospheric due to pressure drop through the catalyst bed. When the CO pretreatment was completed, a passivating gas (2% oxygen in nitrogen) was passed over the catalyst at approximately the same flow rate at room temperature for a 48 hour period. A portion of the pretreated/passivated catalyst was then transferred to a 500 mL glass jar containing enough oil (Shell decene trimer) to produce a catalyst concentration of 20

wt.%. The catalyst/oil slurry was placed on a rotated mill and rolled at about 135 rpm for the duration of the study.

At 24, 120, 288, 456 and 900 hours, the jar was removed from the roller and approximately 5g of the catalyst/oil slurry was collected. The jar was then resealed and returned to the roller mill. The 5g sample was washed with tetrahydrofuran, filtered and submitted to particle size/distribution analysis.

A Hitachi S-2700 scanning electron microscope (SEM) was used to obtain the particle size distributions and morphology (VI.9.11). The operating voltage was 20 kV. Scotch tape was placed on an aluminum holder and the washed catalyst powder was mounted directly on the scotch tape. The sample was coated with carbon to minimize the charging effects in the SEM.

Particle size measurements were also performed using a Granulometer-715*, which uses a laser beam to detect the particle size ranges. A water suspension was prepared using a few grams of the catalyst and a few drops of aerosol OT-100 as a dispersant; this was placed in a sample chamber. The water suspension was agitated for about 1 minute and then the suspension was pumped past a window where the laser beam is used to define the particle size range and this is assigned to channels of precalibrated size ranges. The output from the computer provides a plot of the cumulative frequency versus particle size.

Particle size measurements were also carried out using an optical microscope. The sample was mixed with an epoxy resin, formed to a cylindrical shape and, after setting, the end of the cylinder was polished. The polished sample was mounted onto

---

* Manufactured by CILAS.

an optical microscope and the particle size data were collected using a computer connected to the microscope. The data are corrected following the approach used in petrography; thus, the apparent diameter is equal to (π/4) (true diameter) for spherical particles (VI.9.12).

VI.9.3. RESULTS AND DISCUSSION

A scanning electron micrograph from a sample that was rolled for 24 hours is shown in Figure VI.9.1a. The particle size distribution (Figure VI.9.1b) indicates that the major fraction of particles lies in the range of 30-60 μm and the particles are spherical in shape. The data for the carbided sample after 24 hours of rolling are essentially the same as for the calcined catalyst prior to the carbiding step. Micrographs obtained from the sample that was rolled for 120 hours revealed characteristics similar to the 24 hour sample, and there is not a significant variation in particle size distribution or shape (Figure VI.9.2). However, the micrograph (Figure VI.9.3) for the sample that was rolled for 288 hours shows that the major fraction of particles lies in the size range of 10-50 μm. Rolling for 456 hours resulted in a further reduction of particle size (Figure VI.9.4). It is evident that prolonged rolling of the carbided sample in C_{30} oil caused a reduction in the particle size. While the spherical shape morphology is maintained, the spherical particle size is reduced during rolling.

It appears that reasonable attrition data can be obtained from these rolling experiments; however, the attrition is sensitive to experimental conditions. The large batch of catalyst/oil slurry was stored in a sealed container in a refrigerator. The data shown in Figures VI.9.1 through VI.9.4 was obtained by carrying out the rolling with a particular mill using a portion of the catalyst/slurry that had not been stored. After

obtaining the plot shown in Figure VI.9.9, it was desirable to obtain data for a sample that had been rolled for longer times. Insufficient material remained of the sample that had been used to generate the data shown in Figures VI.9.1 through VI.9.5. Thus, another portion of the master catalyst/oil sample was taken and added to a jar which was then rolled for 912 hours. However, the master sample had been stored for about 6 months before the portion used to roll for 912 hours was taken. Following 912 hours of rolling of the aged sample, the particle size did not show the anticipated decrease. Presumably, partial oxidation of the sample during storage had increased the resistance of the particles to attrition.

The preparation of the specimen for SEM examination has a great influence on the resulting particle size. A portion of the catalyst sample that had been rolled for 24 hours was dispersed in absolute ethanol and ultrasonically agitated for 15 minutes. Then the catalyst was collected by filtration and these powders were sprayed onto a scotch tape and carbon coated. A micrograph from this sample is presented in Figure VI.9.5b. It is evident that the spherical particle morphology (Figure VI.9.5a) has been destroyed by ultrasonic agitation of the catalyst prior to the SEM analysis. Hence, the significant difference in particle size of the samples shown in Figures VI.9.5a and VI.9.5b is caused by the sample preparation.

Particle size measurements were also carried out using a granulometer, wherein the particles were agitated ultrasonically and the sizes were determined using a laser. The relationship between the cumulative frequency and the particle diameter as measured by granulometry 1 min. agitation and by SEM for the catalyst which was rolled for 24 hours are presented in Figure VI.9.6. The distributions are similar except

that the data obtained by the granulometry measurements show a much greater amount of particles in the 0-30 μm size range. It appears that the ultrasonic agitation has caused the production of catalyst fines that are measured by the granulometry procedure. The granulometer data for the 24 hour and 456 hour rolled samples are presented in Figure VI.9.7. The 24 hour sample was ultrasonically agitated for 60 seconds in a bath containing water and the dispersant, whereas the 456 hour sample was agitated for only 10 seconds in the sample chamber of the granulometer. Consequently, the particle size for the 456 hour sample appears to be larger than the 24 hour sample. Hence, the sample preparation prior to particle size analysis influence the resulting particle size data.

Particle size measurements were also done using an optical microscope. The catalyst powders were dispersed in a plastic and formed in a mold to produce a cylindrical shape. The plastic specimen was polished prior to mounting the specimen into the optical microscope. Catalyst particle sizes were measured from about 500 particles. The particle size distributions obtained from the 24 hour sample using the optical microscope are presented in Figure VI.9.8. Polishing will not expose each particle at a uniform depth; thus, a correction must be made for the bias introduced by exposing particles that have been polished to varying depths. For spherical particles the true diameter is $4/\pi$ times the apparent (measured) diameter (VI.9.12). The major fraction of particles are in the range of 40-60 μm in diameter, which is in good agreement with the SEM analysis.

A Bühler Micromet 2 (microhardness tester) instrument was used in an attempt to measure the hardness of the carbided iron catalyst. However, the particles were so

soft that the pin penetrated and destroyed the particle even when the lowest weight load was used. Thus, the hardness could not be measured using this technique.

The results in this investigation clearly demonstrate the fact that the sample preparation may have a significant influence on the resulting particle size data. The rolled specimens yielded spherical shape morphology consistently whereas the samples ultrasonically agitated even for 10 seconds completely destroyed the spherical shape morphology. Hence, a reliable particle size analysis must involve a technique with a minimum interference to the original particle size and shape. Sample preparation involving ultrasonic vibration or agitation of the sample powders has been found to completely alter the resulting particle size data.

In Figure VI.9.9, particle diameter is plotted as $1/d^3$ against rolling time. The particle diameter and the volume of the particle appear to change linearly with rolling time. Due to rolling, attrition among the particles causes the reduction in the mean particle diameter.

VI.9.3.a. Particle Size Analysis

Particle size distributions obtained from the catalyst samples rolled for different hours fit the Weibull Probability Function, which can be used for both cumulative size distributions and the corresponding relative frequency distributions (VI.9.13). This method was used to compute the relative frequency distributions and to compare this to the experimental particle size data. Fang et. al. (VI.9.14) recently used this Weibull Distribution Function to describe tungsten particles in a sintered W-14Ni-GFe sample.

The Weibull probability function (VI.9.13) can be expressed as:

$$f(\chi) = \frac{\beta}{\gamma}(\chi-\alpha)^{\beta-1}\exp\left[-\frac{(\chi-\alpha)^{\beta}}{\gamma}\right] \qquad \text{[VI.9.1.]}$$

where α = constant parameter that determines the shift of the distribution relative to the origin.

β = Weibull Modulus, which is an inverse description of the variability of the size about the mean value.

γ = Scaling factor, which is a function of standard deviation and β.

This function yields a cumulative distribution of $N_>$, the number of particles per unit volume larger than size 'χ':

$$N_> = N\exp\left[-\frac{(\chi-\alpha)^{\beta}}{\gamma}\right] \qquad \text{[VI.9.2.]}$$

The term $N_>/N$ yields the cumulative function giving the mean value (m) and standard deviation (σ). The relationship between cumulative fraction and the particle diameter is plotted in Figure VI.9.10 for the 24 hour rolled sample. The fitted and experimental data correlate very well. The mean and standard deviation values thus obtained are utilized in solving eq. [VI.9.1] and the result is the solid line curve in Figure VI.9.11. The mean standard deviations and 'n' are tabulated in Table 1 for the samples.

The data show that the carbided, unsupported iron FTS catalyst is subject to attrition under agitation conditions similar to those expected for operation in a slurry phase reactor. It appears that the size decrease occurs due to attrition rather than fracture of the particle since the smaller particles retain a spherical shape. The calcined catalyst produced less than 5% fines in a test used to measure the attrition

resistance of FCC cracking catalyst. The pyrophoric nature of the carbided catalyst precluded using this test so that a direct comparison of the calcined and the carbided samples could be made. However, it is certain that the carbided sample is much less resistant to attrition than the calcined precursor material. The data indicate that the unsupported iron catalyst produces a carbided material that will attrite rapidly during use in a slurry phase reactor just from the mixing motion in the reactor and independent of changes introduced by the reaction of CO and H_2.

VI.9.4. ACKNOWLEDGMENT

The authors acknowledge the financial support of this work by the Department of Energy contract No. DE-AC22-91PC90056 and by the Commonwealth of Kentucky.

VI.9.5. REFERENCES

VI.9.1. E. A. Barringer and H. K. Bowen, *J. Am. Ceram. Soc.*, **65**, C199 (1982).

VI.9.2. T. Ogihara, H. Nakajima, T. Yanagawa, N. Ogata and K. Yoshida, *J. Am. Ceram. Soc.*, **74**, 2263 1991).

VI.9.3. Y. Oda and J. Ogawa, *Am. Ceram. Soc. Bull.*, **70**, 963 1991).

VI.9.4. K. T. Scott, in "British Ceramic Proceedings," No. 34, R. Morrell and M. G. Nicholas, eds.), British Ceramic society, 1984, p. 195.

VI.9.5. R. Sivakumar and S. V. Joshi, *Trans. Ind. Ceram. Soc.*, **50**, 1 1991).

VI.9.6. I. Kvernes, E. Lugscheider and Y. Lindblom, in "Proceedings of the Second European Symposium on Engineering Cermaics," London, November, 1987, F. L. Riley, ed.), Elsevier, Barking, 1989, p. 45.

VI.9.7. A. T. Ashcroft, A. K. Cheetham, P.J. F. Harris, R. H. Jones, S. Natarajan, G. Sankar, N. J. Stedman and J. M. Thomas, *Catal. Lett.*, **24**, 47 1994).

VI.9.8. R. Srinivasan, L. Rice and B. H. Davis, *J. Am. Ceram. Soc.*, **73**, 3528 1990).

VI.9.9. B. S. Claussen and H. Topsoe, *Catal. Today*, **9**, 189 1991).

VI.9.10. G. Sankar, J. M. Thomas, D. Waller, J. W. Couves, C. R. A. Catlow and G. N. Greaves, *J. Phys. Chem.*, **96**, 7485 1992).

VI.9.11. R. Srinivasan, R. L. Spicer, L. Xu, F. Tungate, R. Gonzalez and B. H. Davis, *J. Mater. Res.*, in press.

VI.9.12. J. Hower, personal communication.

VI.9.13. N. L. Johnson and S. Kotz, Continuim Unvariable Distributions - 1, Houghton Mufflin, Boston, pp. 250-271 1970).

VI.9.14. Z. Fang, B. R. Patterson, and M. E. Turner, Jr., *Mater. Character.*, **31**, 177, 1993).

Table VI.9.1

Mean and Standard Deviation Obtained Using Weibull Probability Function

Rolling Time (Hr)	Mean (μm)	Standard Deviation σ	n
24	50.06	10.727	3.856
120	50.12	10.835	3.986
288	35.20	8.545	2.852
456	25.56	7.245	2.542

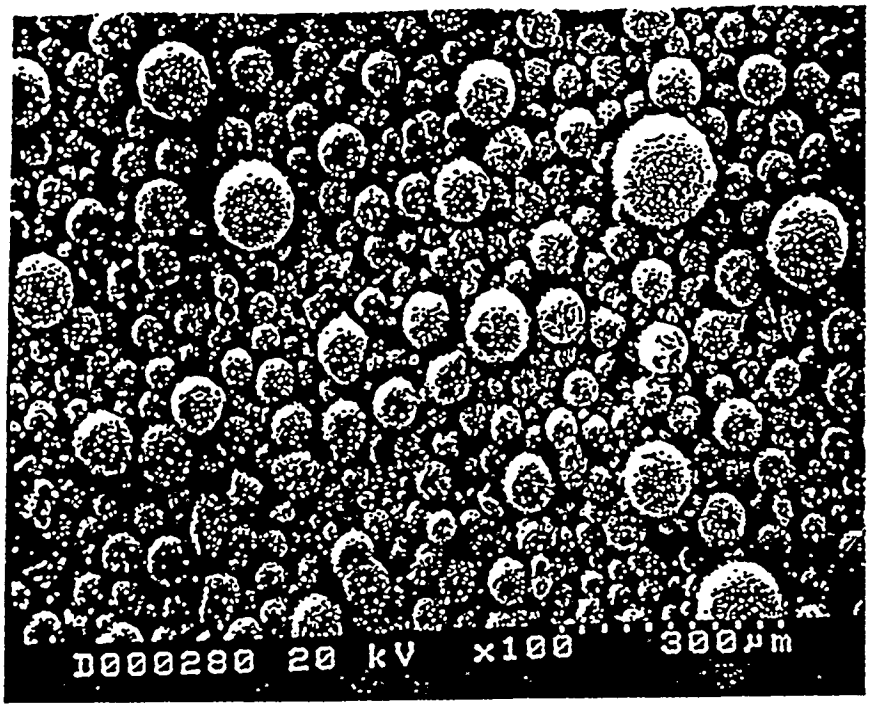

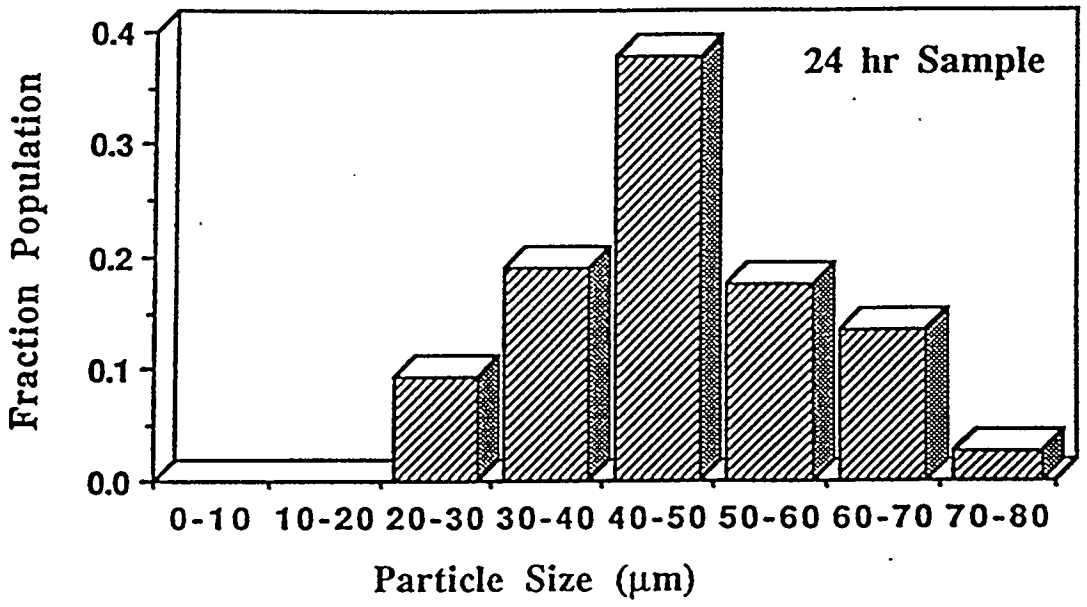

Figure VI.9.1. a) Scanning electron micrograph from the sample rolled for 24 hours. b) Plot of fraction population versus particle size μm). The solid curve is the fitted line using eq. 1).

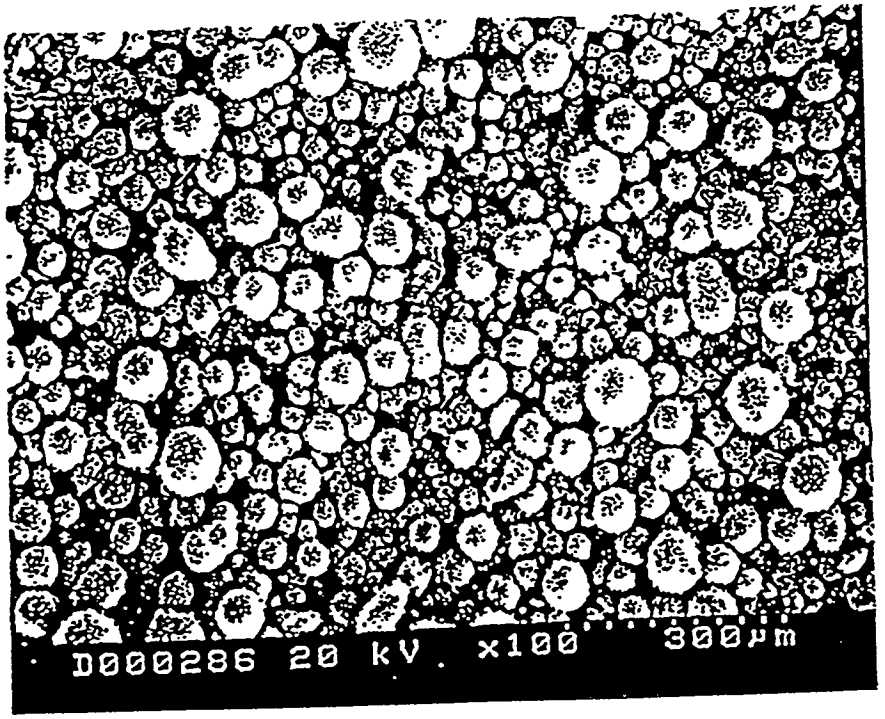

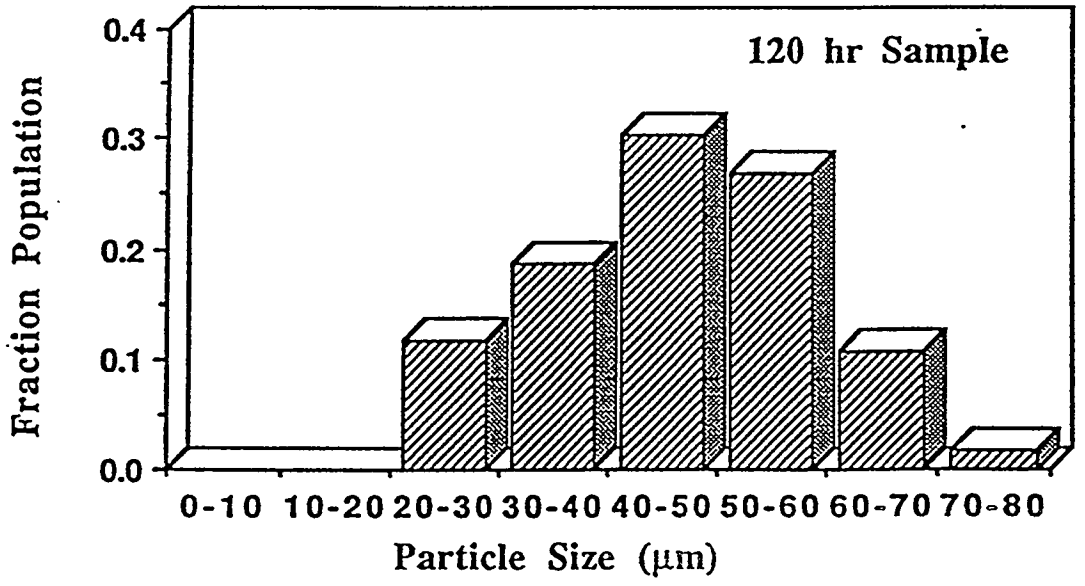

Figure VI.9.2. A scanning electron micrograph from the sample rolled for 120 hours.

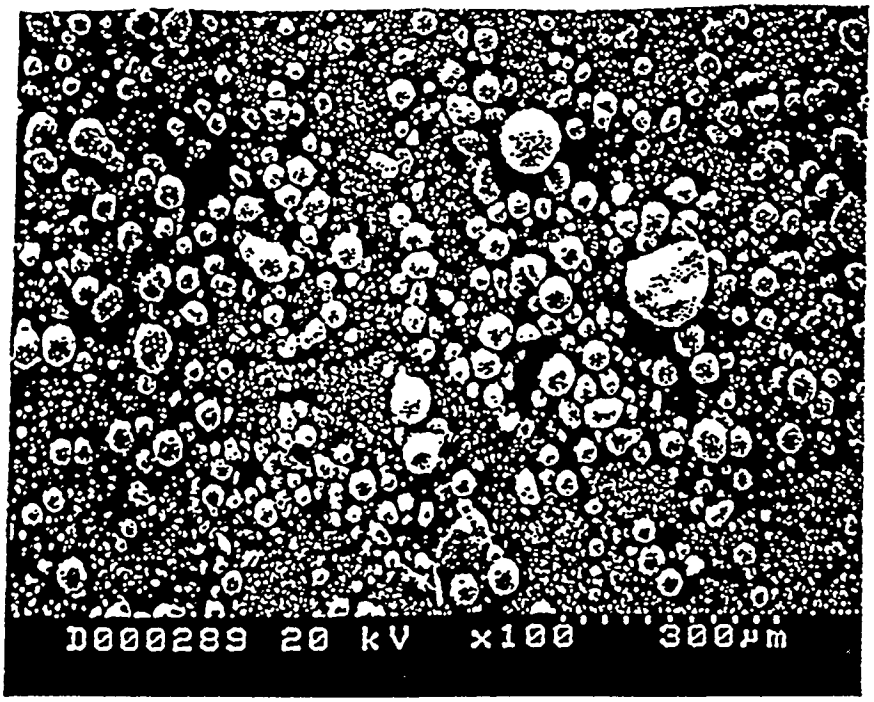

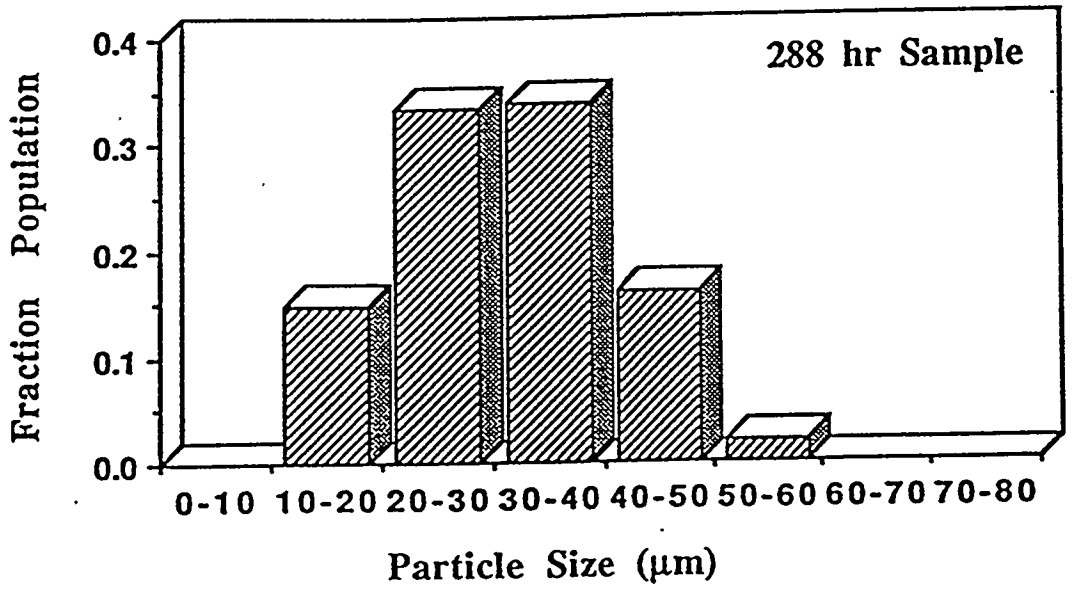

Figure VI.9.3. A scanning electron micrograph from the sample rolled for 288 hours.

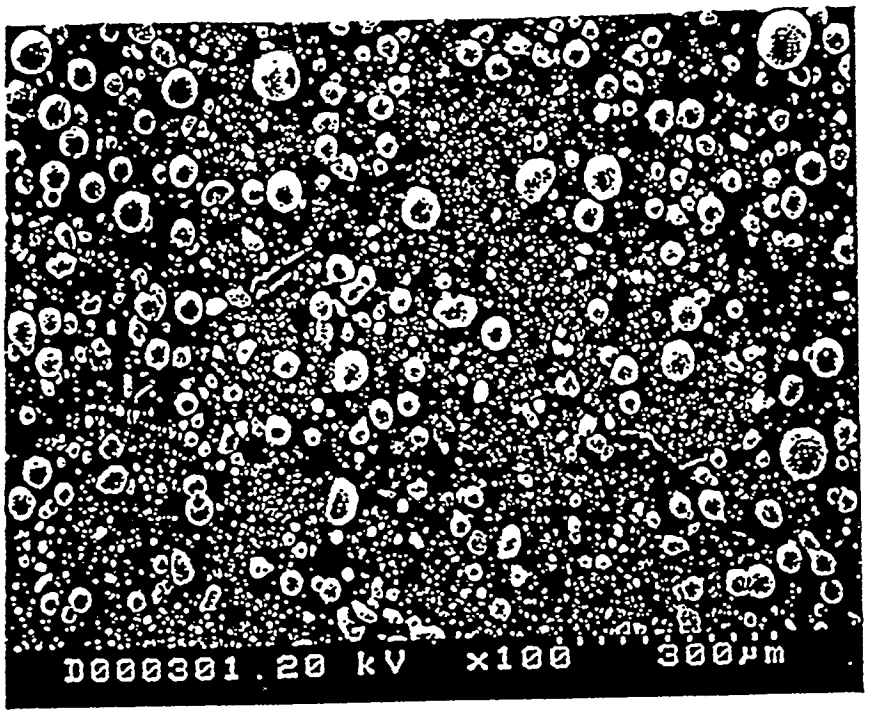

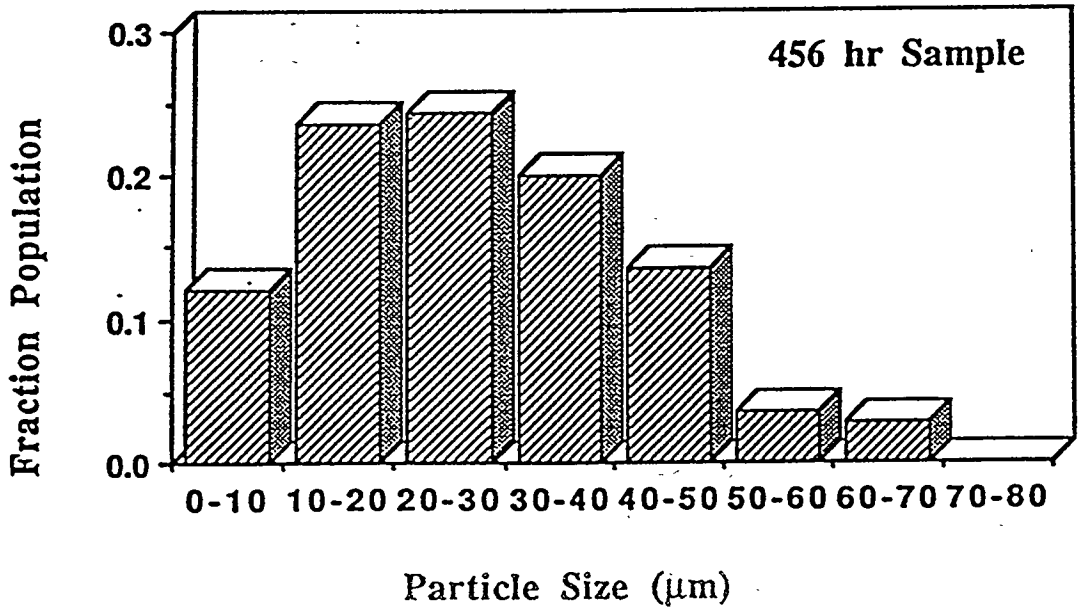

Figure VI.9.4. A scanning electron micrograph from the sample rolled for 456 hours.

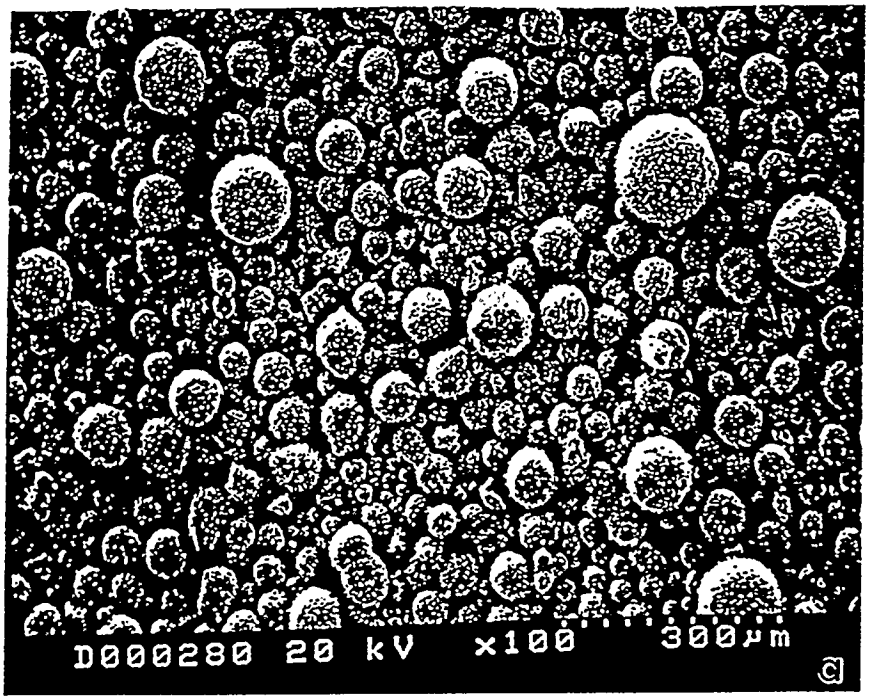

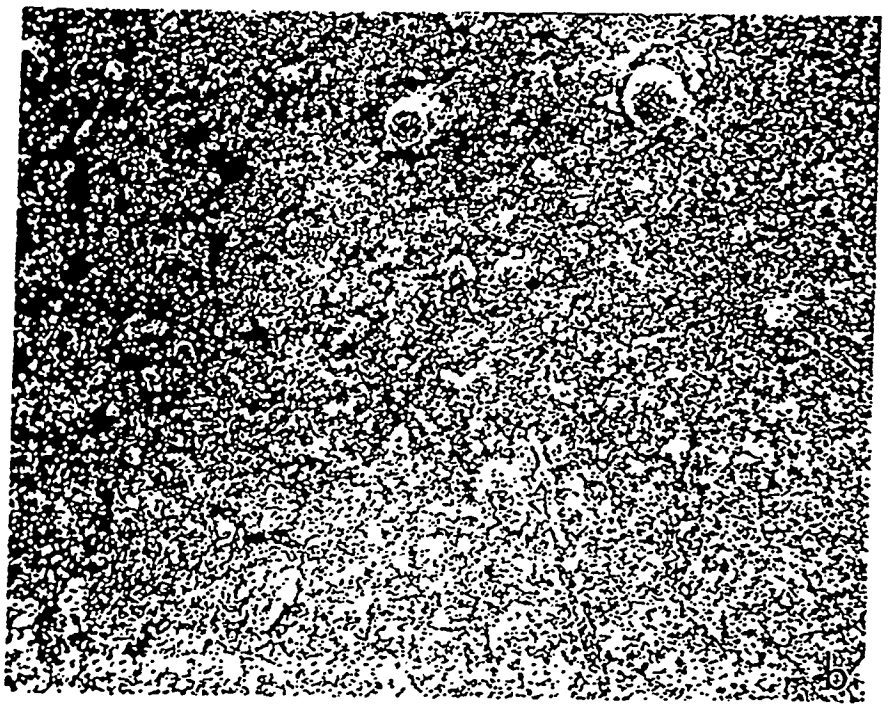

Figure VI.9.5. Scanning electron micrographs obtained from the sample rolled for 24 hours. a) Sample was prepared as rolled. b) Sample was prepared after ultrasonically agitated for 10 minutes. Note the complete destruction of particle morphology.

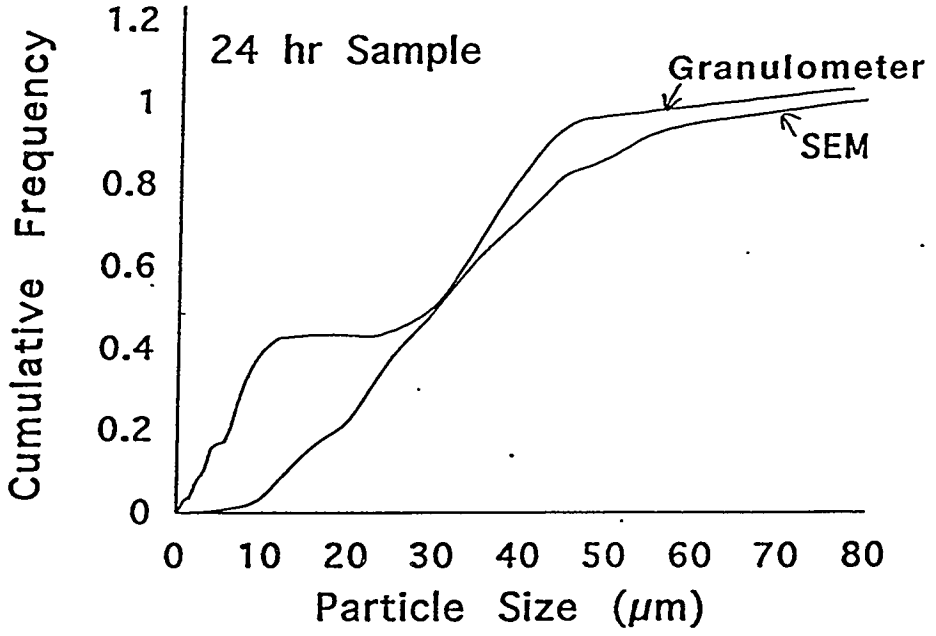

Figure VI.9.6. Cumulative frequency versus particle size plot for the sample rolled for 24 hours. a) From SEM analysis. b) From granulometer analysis.

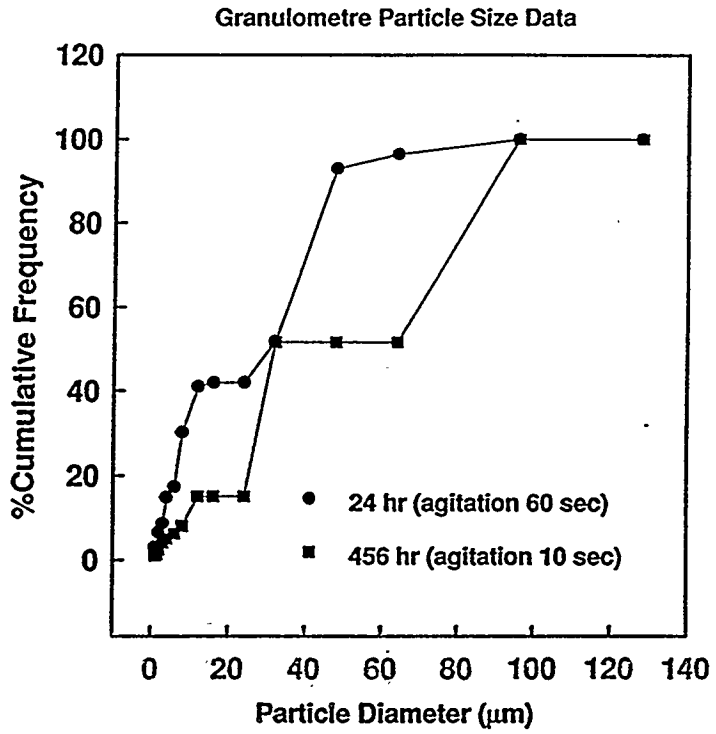

Figure VI.9.7. Particle size data from granulometer analysis. a) Twenty-four hour rolled sample ultrasonic agitation = 60 sec.). b) Four hundred fifty-six hour rolled sample ultrasonic agitation = 10 sec.).

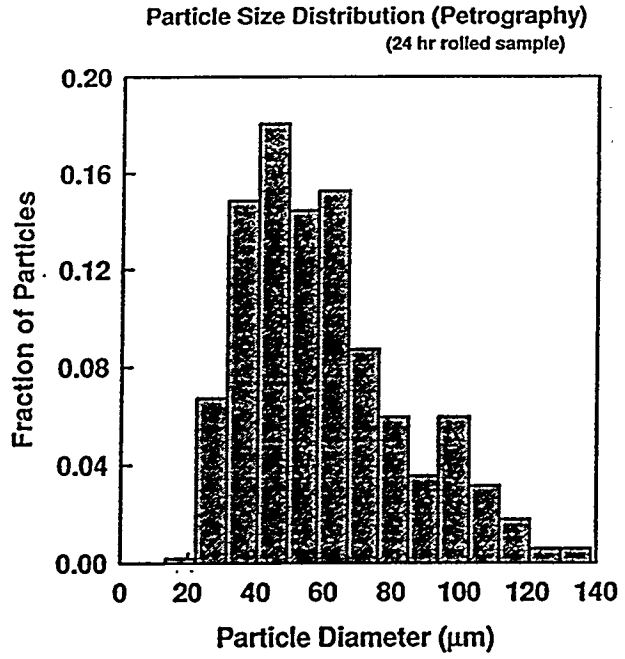

Figure VI.9.8. Particle size distribution for the 24 hour rolled sample. This data were obtained from optical microscopy petrography). Comparable to the data obtained from SEM.

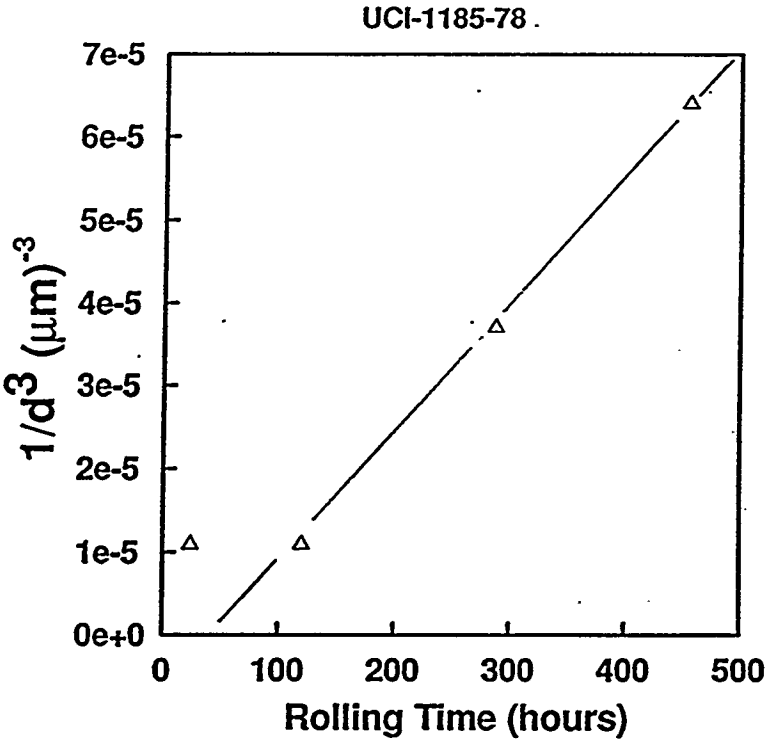

Figure VI.9.9. The plot of $1/d^3$ versus rolling time.

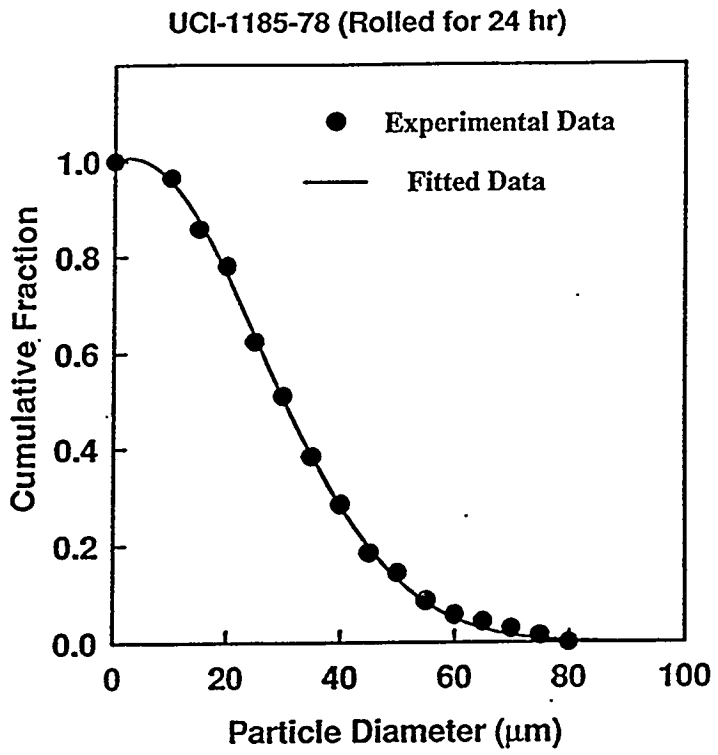

Figure VI.9.10. Cumulative fraction versus particle diameter for the 24 hour rolled sample.

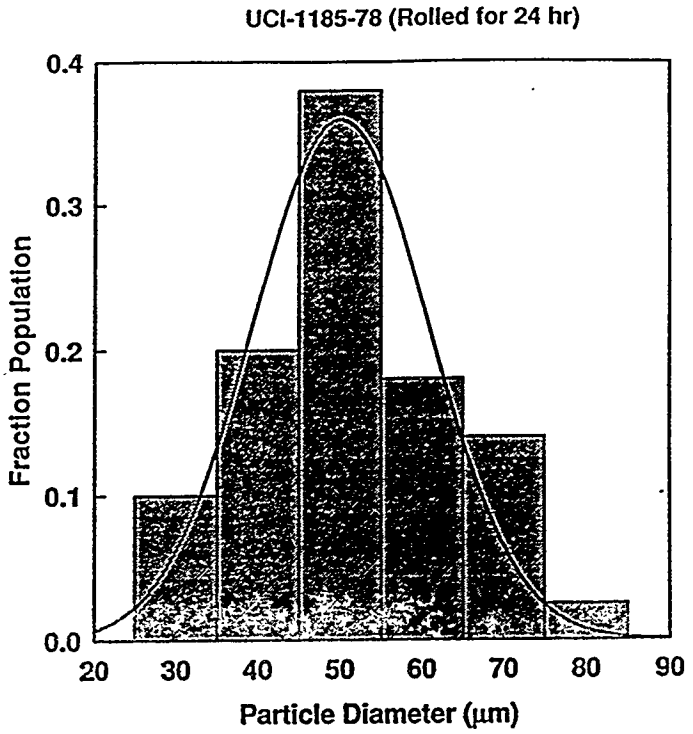

Figure VI.9.11. Fraction population versus particle diameter. The solid line show the fitted curve.